Mathematics and Computers in Simulation XXV (1983) 259–267
North-Holland

A HOLISTIC APPROACH TO VEHICLE SIMULATION

J.N. HOOKER, A.B. ROSE and G.F. ROBERTS

Oak Ridge National Laboratory, Regional and Urban Studies Section, Energy Division, Oak Ridge, TN 37830, U.S.A.

Vehicle simulators traditionally model a vehicle's components separately. This paper describes a "holistic" simulator that constructs a map of fuel consumption vs speed, acceleration, and gear for the vehicle as a whole, based on statistical analysis of road test data. A single computer routine can simulate any number of existing vehicles, once each is outfitted with instruments and a data logger and is tested 1 to 2 days on the road and perhaps on a chassis dynamometer. Results of simulating a 1979 Ford Fairmont station wagon are presented.

1. INTRODUCTION

Vehicle simulators traditionally model a vehicle's components separately. Computer routines or models representing the several components are then linked so as to simulate the behavior of the vehicle as a whole. Such a simulator may be described as *modular* [e.g., 1–4].

This paper describes a different, *holistic* approach to vehicle simulation. In this approach, an existing vehicle whose behavior is to be simulated is driven over a test track while several thousand readings of vehicle speed, acceleration, fuel flow rate, etc., are taken electronically. The data are recorded on magnetic tape and later used to construct a performance map for the vehicle as a whole in roughly the way that one constructs a performance map for an engine. The performance map (usually fuel flow vs speed and acceleration) is approximated as a piecewise polynomial surface and stored as polynomial coefficients, so that computer simulation is little more than table lookup and polynomial evaluation. This approach is holistic in that the automoble is viewed as a whole, rather than as a system of components.

A holistic simulator has the obvious drawback that it cannot be used to simulate a hypothetical vehicle. But when one wishes to simulate existing vehicles that are available for testing, the holistic approach has a number of advantages.

1. Because the vehicle is treated as a black box, a single computer routine can "learn" the performance characteristics of any vehicle whatever.

2. Because simulation is reduced to table lookup and polynomial evaluation, the simulator runs extremely fast.

3. Modular simulators require that performance data be collected on the many components of each vehicle considered, and these data may be difficult to obtain. A holistic simulator requires data only on one component, the vehicle itself, and with the help of an electronic data logger the necessary data can be collected in a few hours on a test track.

4. Holistic simulation results are based on measurements taken in an actual vehicle on the road, rather than on laboratory testing of individual components that may behave differently under road conditions or whose interaction may not be properly accounted for. The number of measurements is large enough that statistical confidence bounds can be estimated.

This paper describes a holistic simulator developed at Oak Ridge National Laboratory to predict automotive fuel economy. This simulator has assisted an investigation of the effect of driver behavior on fuel economy. One aim of the investigation was to determine the optimal control of vehicle speed and gearshift for fuel economy while achieving certain other goals [5]. For instance, one may wish to know the optimal way to drive over a hill while achieving a stated average speed. Optimal control was determined by a dynamic programming routine that obtains fuel flow values from a vehicle simulator. Because the dynamic program drives the simulated vehicle a distance equal to several thousand trips over the stretch of road in question, a very fast simulator was needed. Furthermore, as it was desired to determine optimal control for several existing vehicles on a limited budget, the ability to simulate several vehicles without having to build several simulators was required. A holistic simulator has met these needs well.

The simulator's overall structure is described below. Subsequent sections deal with data

0378-4754/83/$3.00

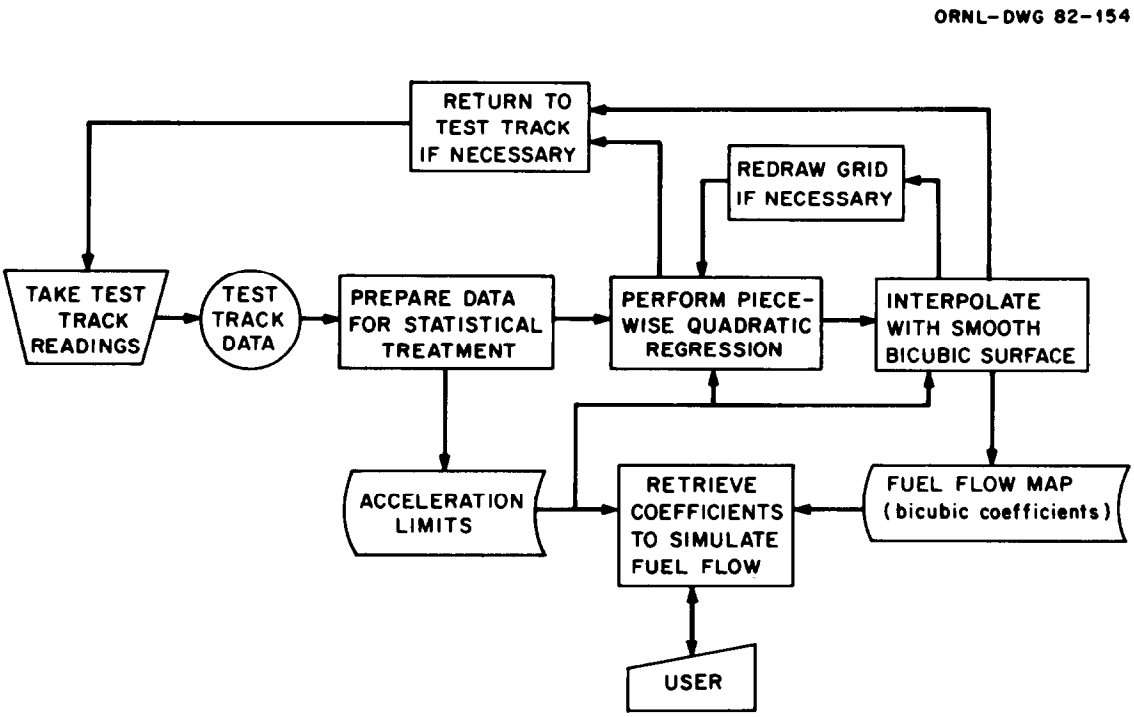

Fig. 1. Overall procedure for simulation of a vehicle's fuel economy.

preparation, statistical testing, smooth surface interpolation, retrieval, and performance to date.

2. OVERVIEW

Figure 1 depicts the overall procedure by which simulation of a given vehicle is achieved. Nearly simultaneous observations of vehicle speed, acceleration, and fuel flow rate are taken electronically on the track while the driver achieves a wide range of speeds and acceleration. (Instantaneous fuel flow rates are inferred from observations of engine speed and intake manifold vacuum, as described in Sect. 10.) The observations are recorded on a magnetic tape cartridge and later transferred to a computer, where they are prepared for statistical treatment.

Next, a plane representing speed vs acceleration is overlaid with a rectangular grid. The adjusted observations of fuel vs speed and acceleration in and surrounding each rectangle are fitted with a small quadratic surface that covers the rectangle; this results in a piecewise quadratic surface over the entire grid. Each regression is subjected to tests to gauge the variability in the data.

Once all statistical tests have been passed, each fitted quadratic is used to calculate a predicted fuel flow rate at the center of its rectangle. Cubic splines are run through these calculated points, resulting in a smooth piecewise bicubic surface. Another statistical test is run to determine whether the interpolated cubic and fitted quadratic surfaces diverge too greatly at the corners of the rectangles.

The simulation itself is performed by a relatively short routine. Given a desired speed, acceleration, and gear, the simulator retrieves the coefficients of the appropriate bicubic polynomial and calculates the corresponding rate of fuel flow.

The problem underlying this holistic approach to simulation is that of generating a *smooth* fuel flow surface while simultaneously performing statistical tests of *error*. This difficulty was resolved by adopting a two-stage procedure; first a piecewise polynomial regression to estimate error, and then a smooth interpolation of poles obtained from the fitted polynomials.

3. COMPUTING EFFECTIVE ACCELERATION

The magnitude of the acceleration relevant to determining the load on the engine (i.e., the effective acceleration) is

$$a = \dot{v} + g \sin\theta + r , \qquad (1)$$

where $\dot{v}$ is the magnitude of the kinetic acceleration of the vehicle in the direction of its motion, g the acceleration due to gravity, θ the angle of the road slope, and r the result of rotational inertia of the drive train. Testing was performed on a level track, so that $\theta = 0$, and $\dot{v}$ was deduced from the angle ϕ of apparent inclination as measured by an inclinometer in the car. (Acceleration readings obtained by differentiating the speed signal from the fifth wheel contained excessive noise.) Since $\tan\phi = \dot{v}/g$, (1) can for a level track be written

$$a = g \tan\phi + r . \qquad (2)$$

The acceleration r due to rotational inertia is approximately $\gamma_u \dot{v}$, where γ_u is a constant that is characteristic of the gear u. For simplicity r was ignored during the construction of the performance map. The resulting map therefore provides for each gear u a function $f_u(v, a)$ that delivers the fuel flow rate for speed v and effective acceleration $a(1 + \gamma_u)$ on a level road. If the car is moving at speed v on a grade of angle θ, then from (1) the effective acceleration is $a = (1 + \gamma_u)\dot{v} + g \sin\theta$, and the fuel flow rate in gear u is

$$f_u[v, a/(1 + \gamma_u)] = f_u\left(v, \dot{v} + \frac{g \sin\theta}{1 + \gamma_u}\right) . \qquad (3)$$

The constant γ_u is negligible other than in first gear.

4. ACCELERATION LIMITS

Care is taken during road tests to operate the vehicle at full throttle and to let it coast at many different speeds and in each gear (if it has manual shift). The upper and lower boundaries of the resulting data points plotted on a speed vs acceleration plane respectively define the upper acceleration limits and coasting deceleration of the vehicle at all speeds.

To represent these boundaries mathematically, suppose that the observed speed and acceleration pairs are (v_i, a_i), $i = 0,\ldots, n$, and that $v_0,\ldots, v_n$ (which may be assumed distinct) are ordered by size. The upper boundary is first approximated by an upper piecewise linear hull extending from v_0 to v_n. This hull consists of a series of line segments connecting the points (v_{i_k}, a_{i_k}), $k = 0,\ldots, m$, where

$$\frac{a_{i_{k+1}} - a_{i_k}}{v_{i_{k+1}} - v_{i_k}} = \max_{j \in J_k} \frac{a_j - a_{i_k}}{v_j - v_{i_k}} ,$$

$$k = 0,\ldots, m - 1 ,$$

and where

$$J_k = \{j \mid 0 < v_j - v_{i_k} \leq L\} .$$

L is chosen by eye so that the resulting hull most closely follows the upper boundary. A lower hull is similarly obtained.

The hull is smoothed with a cubic spline in the following way. A series of hull points is obtained by inserting points at fixed intervals along the hull line segments. For each of a series of evenly-spaced speed grid points $\tilde{v}_0,\ldots, \tilde{v}_{n_v}$, the hull points with speed coordinates surrounding $\tilde{v}_i$ are fitted to a quadratic function $q_i(v)$ from which an estimate $q_i(\tilde{v}_i)$ of the maximum acceleration at $\tilde{v}_i$ is obtained. A cubic spline through the points $[\tilde{v}_i, q_i(\tilde{v}_i)]$ is taken to define the maximum or coasting acceleration at each speed. The spline is a piecewise cubic function whose coefficients are calculated according to a formula given in [6], p. 212.

5. THE REGRESSION FUNCTION

It is assumed that the dependence of fuel flow on speed and acceleration is locally quadratic within acceptable tolerances. It is therefore modeled as piecewise quadratic function.

Let $\tilde{v}_0, \tilde{v}_1,\ldots, \tilde{v}_{n_v}$ be evenly-spaced speed grid points with separation $\Delta\tilde{v}$, and $\tilde{a}_0,\ldots, \tilde{a}_{n_a}$ be acceleration grid points with separation $\Delta\tilde{a}$. (The grid points may be different for different gears, although for simplicity the notation does not reflect this.) Define the rectangular area

$$R(k, m, h) = \left\{(v,a) \,\middle|\, |v - \tilde{v}_k| \leq \tfrac{1}{2} h\Delta\tilde{v} , \; |a - \tilde{a}_m| \leq \tfrac{1}{2} h\Delta\tilde{a}\right\} .$$

Then the rate of fuel flow is approximated for each gear u as a piecewise quadratic function $q_u(v,a)$ of speed v and effective acceleration a, where

$$q_u(v, a) = q_{ukm}(v, a) \text{ if } (v, a) \in R(k, m, 1) . \qquad (4)$$

The quadratic functions q_{ukm} are of the form

$$q_{ukm}(v, a) = z(v, a)\beta_{ukm} , \quad (5)$$

where β_{ukm} is a column vector of six coefficients and $z(v, a) = (1, v, v^2, a, a^2, va)$.

6. ESTIMATION OF COEFFICIENTS AND ERROR

The coefficients β_{ukm} in Eq. (5) are estimated as follows. Let $(x_{i_1}, y_{i_1}),\ldots, (x_{i_p}, y_{i_p})$ be the observations in $R(k, m, h)$, where $x_j = (v_j, a_j)$. Also let $X = [z(x_{i_1}),\ldots, z(x_{i_p})]'$, $y = (y_{i_1},\ldots, y_{i_p})'$. It is assumed that $y = X\beta_{ukm} + e$, where the error terms in $e = (e_{i_1},\ldots, e_{i_p})$ are independently and normally distributed, with equal variances, about a mean of zero. Under this assumption an unbiased maximum likelihood estimate of β_{ukm} is given by the least-squares formula

$$\hat{\beta}_{ukm} = (X'X)^{-1}X'y . \quad (6)$$

Confidence bounds on the estimate provided by Eq. (5) can be obtained as follows. Let the predicted fuel flow at $x = (v, a)$ be $\hat{y} = z(x)\hat{\beta}_{ukm}$. If

$$s = \left[\sum_{j=1}^{p} e_{ij}^2/(p - 6)\right]^{1/2} ,$$

then a 100 $(1 - \varepsilon)$ % confidence interval for $\hat{y}$ is

$$\hat{y} \pm t_{\varepsilon/2}\, s[z(x)'(X'X)^{-1}z(x)]^{1/2} \quad (7)$$

where t represents the t distribution with $p - 6$ degrees of freedom.

The width of the confidence interval (7) is taken as a measure of the accuracy with which fuel flow can be estimated. The interval width is checked at all grid points $(\tilde{v}_k, \tilde{a}_m)$.

7. SMOOTH SURFACE INTERPOLATION

The piecewise quadratic regression described in the previous sections yields estimates of fuel flow rate at evenly spaced points (poles). The present task is to find a smooth surface that interpolates these poles. Bicubic spline interpolation has proved a useful technique for obtaining such a surface [6–11].

For each gear the poles to be interpolated are all the points $(\tilde{v}_k, \tilde{a}_m, \tilde{y}_{km})$, where $\tilde{y}_{km} = z(\tilde{v}_k, \tilde{a}_m)\hat{\beta}_{ukm}$, except for those points that lie well outside the acceleration limits of the vehicle. (It is usually necessary to include some poles just beyond the limits so as to complete the surface within the limits.) The piecewise bicubic interpolating function $b(v, a)$ will estimate fuel flow

$$f_u(v, a) = b(v, a) , \quad (8)$$

where

$$b(v, a) = b_{km}(v, a) \text{ if } \tilde{v}_{k-1} \leq v \leq \tilde{v}_k \text{ and } \tilde{a}_{m-1} \leq a \leq \tilde{a}_m , \quad (9)$$

and where

$$b_{km}(v, a) = \sum_{i=0}^{3}\sum_{j=0}^{3} \gamma_{ijkm} v^i a^j . \quad (10)$$

The interpolation technique of de Boor [6] was found satisfactory, even though it is designed for a rectangular grid. The set T of poles to be interpolated do not in general form a rectangular grid, since fuel flow estimates are provided only for points within or near the acceleration limits of the vehicle. De Boor's technique is therefore adapted below to any *rectangularly convex* array of poles. A set S of grid points is here defined to be rectangularly convex if $(\tilde{v}_k, \tilde{a}_m) \in S$ whenever $(\tilde{v}_{k_0}, \tilde{a}_m) \in S$, $(\tilde{v}_{k_1}, \tilde{a}_m) \in S$, and $k_0 \leq k \leq k_1$, as well as whenever $(\tilde{v}_k, \tilde{a}_{m_0}) \in S$, $(\tilde{v}_k, \tilde{a}_{m_1}) \in S$, and $m_0 \leq m \leq m_1$. It is necessary to choose manually from T a rectangularly convex set S of grid points, usually as large a set as possible. Interpolation over S is dealt with first below, and then interpolation over the rest of T.

De Boor's procedure, amended for present purposes, is to pass cubic splines through the given poles along the coordinate lines $v = \tilde{v}_k$ and $a = \tilde{a}_m$. The regression functions (6) supply the slopes at the endpoints of the splines as well as second derivatives at all poles. The piecewise bicubic function b, then, must satisfy the conditions

$$b(\tilde{v}_k, \tilde{a}_m) = \tilde{y}_{km} = b_{km}, \quad k = n_{vm},\ldots, n'_{vm}, \quad m = 0,\ldots, n_a ,$$

$$b^v(\tilde{v}_k, \tilde{a}_m) = q^v_{ukm}(\tilde{v}_k, \tilde{a}_m) = b^v_{km}, \quad k = n_{vm}, n'_{vm}, \quad m = 0,\ldots, n_a ,$$

$$b^a(\tilde{v}_k, \tilde{a}_m) = q^a_{ukm}(\tilde{v}_k, \tilde{a}_m) = b^a_{km} \quad m = n_{ak}, n'_{ak}, \quad k = 0,\ldots, n_v ,$$

$$b^{va}(\tilde{v}_k, \tilde{a}_m) = q^{va}_{ukm}(\tilde{v}_k, \tilde{a}_m) = b^{va}_{km}, \quad k = n_{vm},\ldots, n'_{vm}, \quad m = 0,\ldots, n_a ,$$

where

$$n_{vm} = \min\{k \mid (\tilde{v}_k, \tilde{a}_m) \in S\} ,$$

$$\hat{n_{vm}} = \max\{k \mid (\tilde{v}_k, \tilde{a}_m) \in S\} ,$$

$$n_{ak} = \min\{m \mid (\tilde{v}_k, \tilde{a}_m) \in S\} ,$$

$$\hat{n_{ak}} = \max\{m \mid (\tilde{v}_k, \tilde{a}_m) \in S\} .$$

The superscripts indicate derivatives, with the convention that $g^x(x_o, y_o) = \partial g/\partial x$ evaluated at (x_o, y_o) and $g^{xy}(x_o, y_o) = \partial g^2/\partial x \partial y$ evaluated at (x_o, y_o).

The unspecified first derivatives b^v_{km} and b^a_{km} are obtained by solving the system of linear equations

$$b^a_{k,m-1} + 4b^a_{km} + b^a_{k,m+1} = \frac{3}{\Delta\tilde{v}} (b_{k,m+1} - b_{k,m-1}),$$

$$m = 1, \ldots, n_a - 1 , \quad (11)$$

for each $k = 0, \ldots, n_v$, and the system

$$b^v_{k-1,m} + 4b^v_{km} + b^v_{k+1,m} = \frac{3}{\Delta\tilde{a}} (b_{k+1,m} - b_{k-1,m}),$$

$$k = 1, \ldots, n_v - 1, \quad (12)$$

for each $m = 0, \ldots, n_a$. De Boor (p. 217) presents an efficient technique for solving the tridiagonal systems Eq. (11) and Eq. (12).

The poles define rectangles on the v/a plane, and each rectangle is given a bicubic surface defined by Eq. (10). Once the first and second derivatives at the corner poles of a rectangle are obtained as above, this unique interpolating bicubic is straightforwardly derived as described in [6], p. 215.

It remains to find interpolating surfaces for rectangles with one or more corners in T - S. If a corner of a given rectangle lies in T - S the derivatives at that point are taken to be the corresponding derivatives of q_{uij}. Corners in S are given derivatives as above, and the interpolating bicubic is again determined by the corner derivatives.

8. TESTING THE INTERPOLATING SURFACE

The surface defined above is tied to the underlying fuel flow data only at the poles $(\tilde{v}_k, \tilde{a}_m, \tilde{y}_{km})$. Since the surface between these poles may depart significantly from the data points, it is appropriate to test statistically the hypothesis that the interpolating surface lies within a tolerance δ of the underlying quadratic fuel flow surface at the *corners* of the fitting rectangles. The tolerance δ is permitted because the true fuel flow surface need not be assumed exactly but only approximately quadratic.

The test is carried out by using Eq. (7) to calculate for each grid point $(\tilde{v}_k, \tilde{a}_m)$ the upper and lower bounds B^+ and B^- of the confidence interval at each of the four points

$$x_{ij} = \left(\tilde{v}_k + \frac{1}{2} i\Delta\tilde{v}, \tilde{a}_m + \frac{1}{2} j\Delta\tilde{a}\right),$$

$$i = 1, -1, j = 1, -1 .$$

It is required that

$$B^- - \delta q_{km}(x_{ij}) \leq f_u(x_{ij}) \leq B^+ + \delta q_{km}(x_{ij}) , \quad (13)$$

for each i, j. Generally $\delta = 1\%$ is used. If this test is failed, the grid is made finer or shifted, or else a larger h is used in the fitting procedure. The test is not performed at corners lying outside the acceleration limits.

9. RETRIEVAL

The coefficients of the bicubic polynomials Eq. (10) are packed into core and indexed as follows. The polynomial coefficients for grid point $(\tilde{v}_k, \tilde{a}_m)$ and gear u are stored at location

$$L_{km} + t(u, h_{km}) .$$

Here L is an indexing array generated so that $L_{km} + 1$ is the location of the cubic $f_{u'km}$ corresponding to the lowest gear u' for which a cubic is provided at grid point $(\tilde{v}_k, \tilde{a}_m)$. The array h is in effect a hash function defined

$$h_{km} = 1 + \sum_{u=1}^{n_g} 2^{u-1} d_{ukm}$$

where n_g is the number of gears and where

$$d_{ukm} = \begin{cases} 1 \text{ if cubic } f_{ukm} \text{ is provided,} \\ 0 \text{ otherwise.} \end{cases}$$

Array h is generated along with L. The effect of array t, which is pre-defined, is to group the f_{ukm}'s together for each k, m. In each such group the cubic corresponding to gear u is number $t(u, h_{km})$. More precisely,

$$t(u, h_{km}) = \begin{cases} \sum_{u'=1}^{u} d_{u'km} \text{ if } d_{ukm} = 1, \\ 0 \text{ otherwise.} \end{cases}$$

10. RESULTS

A performance map has been constructed for a 1979 Ford Fairmont station wagon with automatic transmission. The car was equipped with a fifth wheel (to measure speed), an inclinometer, a tachometer, a pressure gauge (for intake manifold vacuum), a fuel flow meter, four thermometers (ambient, oil, water, fuel), and a digital trip recorder. The car has a carburetor, and measurement of fuel flow had to be taken at the bowl intake. Modeling of the bowl's filling failed to yield accurate estimates of instantaneous fuel flow into the engine, partly because the fuel in the bowl is prone to slosh and close the intake valve upon acceleration. The problem was solved by constructing a map of fuel flow vs rpm and manifold vacuum based on steady-state data taken when the car was mounted on a chassis dynamometer, where there was no slosh problem. This dynamometer map was constructed in the same way as the maps showing performance on the road. It was used to replace each rpm and vacuum measurement taken on the road with a simulated fuel flow value. (The dynamometer and on-road testing procedures are described in detail in [12].)

A different on-road performance map was made for each gear, and data for the several gears were segregated primarily on the basis of the vehicle speed/engine speed ratio. This procedure very nearly partitioned the points on the speed vs acceleration plot into three regions corresponding to the three gears.

Figures 2–5 show the statistical results of map construction for the dynamometer and on-road

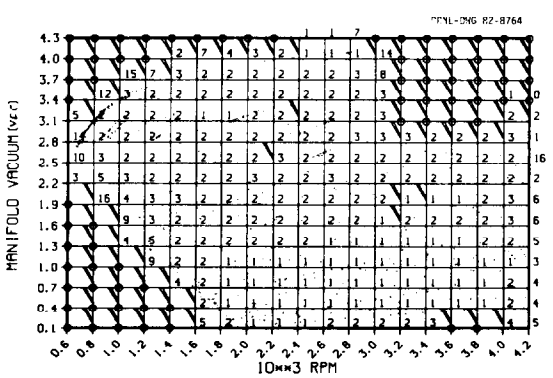

Fig. 2. Statistical results of dynamometer performance map construction for a 1979 Ford Fairmont station wagon with automatic transmission. The intake manifold vacuum values are in uncalibrated voltage readings from the sensor. Large numbers indicate higher vacuum (lower pressure), so that fuel flows are greatest at bottom right. Figures 2–5 are explained in text.

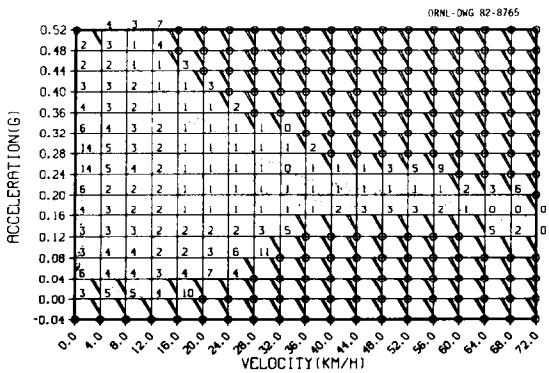

Fig. 3. Statistical results of first-gear on-road performance map construction for the Fairmont.

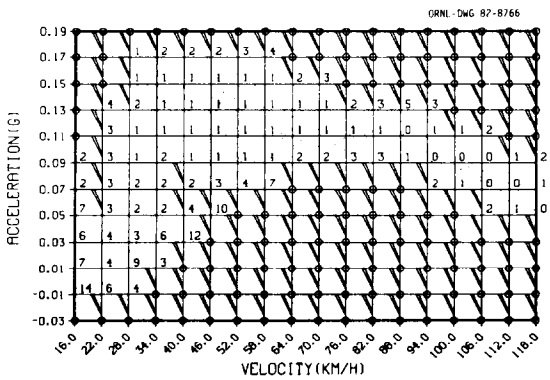

Fig. 4. Statistical results of second-gear on-road performance map construction for the Fairmont.

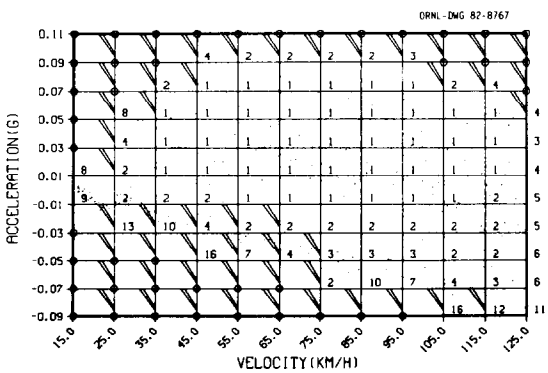

Fig. 5. Statistical results of third-gear on-road performance map construction for the Fairmont.

tests. The scattered points represent observations (789 for gear 1, 686 for gear 2, and 2526 for gear 3). The grid points (corners of the rectangles) are the poles to which the interpolating surface is tied. Each number pertains to the pole at its lower left and is the half-width of a 90% confidence interval calculated by Eq. (7), expressed in percentage points. The small circles mark poles that were not estimated, due either to a lack of data or numerical problems. The diagonal stripes mark rectangles for which satisfactory bicubics were not derived. If one or more of the cubics of a striped rectangle is encircled, then no bicubic is provided. Otherwise, a bicubic is provided but it fails test (15) at a 90% confidence level and a tolerance δ of 1% (3% for the dynamometer map). Aside from those in the dynamometer map, most bicubics that fail this test at a 1% tolerance pass at a 2% or 3% tolerance.

Figures 6–8 show the bicubic interpolating surfaces used for simulation. Only the portion of a surface that lies within the acceleration limit curves is plotted. Occasionally these curves cross the corner of a rectangle for which no bicubic is provided, so that an adjacent bicubic must be extended slightly to complete the surface.

The confidence bands are amply narrow, due partly to the large number of data on which they are based. The interpretation of these results should take into account two caveats, however. Variability in observed fuel flows at a given speed and acceleration cannot be explained simply as resulting from errors in the measurement of a single true fuel flow value. Rather, the performance of the automobile itself varies somewhat at a given speed and acceleration, and this accounts for some of the variability. This means that one cannot be 90% confident that the actual performance of the car at a given speed and acceleration will lie within the stated confidence band on a

ORNL-DWG 82-8769

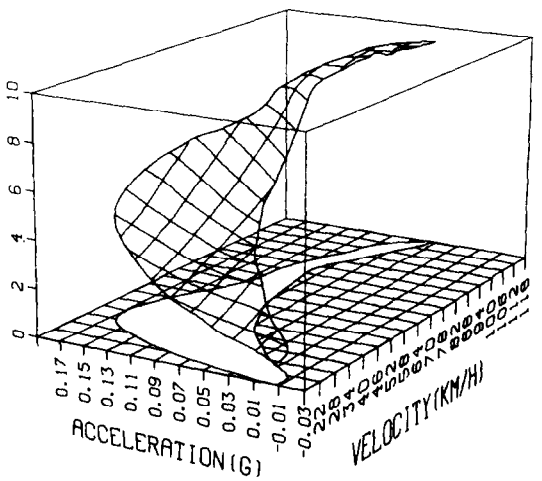

Fig. 7. Fuel flow rate (mL/s) vs speed and acceleration in second gear for the Fairmont.

ORNL-DWG 82-8768

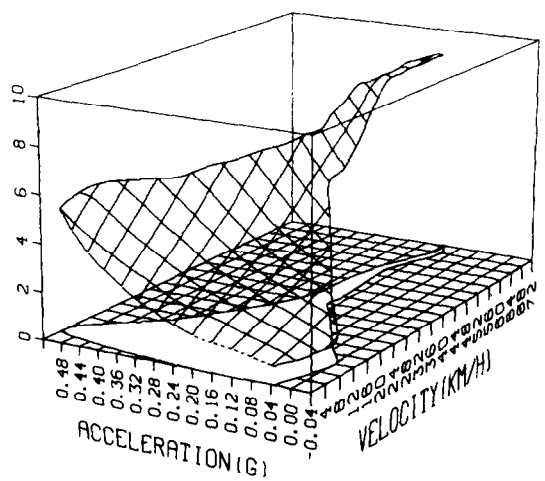

Fig. 6. Flue flow rate (mL/s) vs speed and acceleration in first gear for the Fairmont.

ORNL-DWG 82-8770

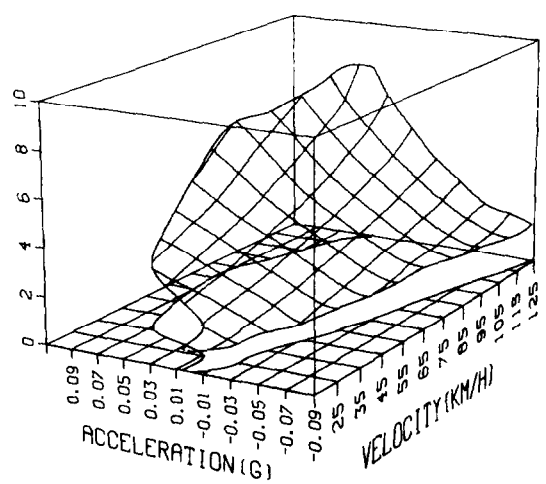

Fig. 8. Fuel flow rate (mL/s) vs speed and acceleration in third gear for the Fairmont.

particular occasion. Yet if the "true" fuel flow about which the observed values are distributed is interpreted as the *average* performance of the car at that speed and acceleration, then one can be 90% confident that this average lies within the confidence band.

The second caveat is that the confidence bands are a reflection only of random variability in the data and would not register any bias in the measurements. A potential for bias lies in the fact that fuel flow is not measured directly on the road but is inferred from the measured engine rpm and manifold vacuum, based on dynamometer tests.

To quantify any bias, total fuel consumption over each of 69 of the longer test runs was calculated on the basis of measured rpm and vacuum. The calculations were compared with the cumulative fuel flow actually measured on the road. The fuel flow measurement was corrected to account for the fact that the level of fuel in the carburetor bowl may have been different at the beginning of a run than at the end. The bowl levels were estimated on the basis of a quadratic function, derived from dynamometer data, that expresses the rate of flow into the bowl as a function of the bowl level. The test runs were assumed to be long enough that fuel sloshing would add only moderate random error to the cumulative fuel flow measurements.

The results of the comparison appear in Table 1, which also compares actual fuel consumption with that predicted on the basis of measured speed and acceleration, using the maps in Figs. 6–8. If a series of test runs, 1,..., n resulted in an actual fuel use F_i and simulated fuel use S_i for each run i, then the "relative cumulative error" is $\Sigma D_i/\Sigma F_i$, where $D_i = S_i - F_i$. The "mean relative error" is $\Sigma(D_i/F_i)/n$, and the "rms (root mean square) relative error" is $[\Sigma(D_i/F_i)^2/n]^{1/2}$.

Note that the total fuel consumption predicted by the dynamometer map is 3.9% below that measured on the road. This means that the dynamometer map should inject about a 4% downward bias into fuel flows simulated on the basis of speed and acceleration. Table 1 shows that the bias actually measured was 3.8%. The rms relative errors reflect the variability in both the dynamometer data (Fig. 2) and the on-road data (Figs. 3–5) as well as errors in on-road fuel flow measurement resulting from fuel sloshing and inaccuracies in the bowl level corrections. It is not unlikely that errors in on-road fuel measurement are as large as errors in simulation.

A Fortran implementation of the simulator was tested on two computers for speed. One thousand computations of instantaneous fuel flow as a function of speed, acceleration, and gear required 0.67s on a DEC-10 computer and 0.21s on an IBM 3033 computer. Ten thousand computations required 5.93 and 1.57s on the two computers, respectively. The time measurements include the overhead required to read the coefficients into core and set up the indexing arrays described in Sect. 9.

11. ACKNOWLEDGMENTS

The research described in this paper was supported as part of the Driver Energy Conservation and Awareness Training program operated by the Department of Energy. The authors were assisted by R. B. Hofstra, D. R. Miller, G. N. Miller, and S. C. Rogers of Oak Ridge National

Table 1. Comparison of simulated and actual fuel consumption over 69 test runs of a 1979 Ford Fairmont station wagon

	All runs	Deceleration	Low acceleration	Medium acceleration	High acceleration
Number of runs	69	13	24	18	14
Mean duration(s)	33	37	39	28	23
Simulation based on rpm and vacuum					
Relative cumulative error (%)	-3.9	-5.0	-5.5	-2.9	-2.3
Mean relative error (%)	-2.9	-4.0	-3.9	-2.0	-1.2
rms relative error (%)	6.5	10.1	6.6	4.0	4.1
Simulation based on speed and acceleration					
Relative cumulative error (%)	-3.8	-5.2	-2.5	-3.3	-3.8
Mean relative error (%)	-2.9	-2.5	-4.0	-2.3	-2.1
rms relative error (%)	6.5	9.1	6.5	5.2	4.5

Laboratory and by J. Hodgson of the Mechanical and Aerospace Engineering Department at the University of Tennessee.

REFERENCES

[1] W. C. Waters, "General Purpose Automotive Vehicle Performance Simulator," SAE paper no. 720043, 1972.

[2] R. K. Louden and I. K. Lukey, "Computer Simulation of Automotive Fuel Economy and Acceleration," paper 196A presented at SAE Summer Meeting, Chicago, June 1960.

[3] N. H. Beachley and A. A. Frank, "Increased Fuel Economy in Transportation Systems by Use of Energy Management," vol. 2: Digital Automotive Propulsion Simulator Programs and Description, prepared for Dept. of Transportation, DOT-TST-75-2, December 1974.

[4] J. M. Wollam, "Generalized Tracked and Wheeled Vehicle Automotive Performance Model," SAE paper no. 710628, June 1971.

[5] J. N. Hooker, A. B. Rose, G. F. Roberts, "Optimal Control of Vehicles for Fuel Economy," to appear in *Transportation Science*, (in press), 1983.

[6] C. de Boor, Bicubic Spline Interpolation, *J. Math. Physics* 41; 212–218 (1962).

[7] J. H. Ahlberg and E. N. Wilson, "Extremal, Orthogonality and Convergence Properties of Multidimensional Splines," *J. of Math. Anal. and Appli.* 12: 27–48 (1965).

[8] P. M. Anselone and P. J. Laurent, "A General Method for the Construction of Interpolating or Smoothing Spline-Functions," *Num. Math.* 12: 83–90 (1968).

[9] M. Atteia, "Existence et détermination des functions spline a plusieurs variables," *C. R. Acad. Sci. Paris* 262: 575–78 (1966).

[10] G. Birkhoff and H. L. Garabedian, "Smooth Surface Interpolation," *J. Math. and Physics* 39: 258–68 (1960).

[11] G. Birkhoff and H. L. Garabedian, "Piecewise Polynomial Interpolation and Approximation," in: Approximation of Functions, H. L. Garabedian, ed., Amsterdam: Elsevier (1965).

[12] A. B. Rose, J. N. Hooker, G. F. Roberts, J. Hodgson, "A Data-Based Simulator for Predicting Vehicle Fuel Consumption," SAE paper no. 820302, 1982.